

Anti-dark soliton complexes in a fiber laser

Xiao Hu,^{a,b} Jun Guo,^c Guangwei Hu,^{a,b} Seongwoo Yoo,^b and Dingyuan Tang^{a,*}

^aShenzhen Technology University, Future Technology School, Shenzhen, China

^bNanyang Technological University, School of Electrical and Electronic Engineering, Singapore

^cJiangsu Normal University, Jiangsu Key Laboratory of Laser Materials and Devices, School of Physics and Electronic Engineering, Xuzhou, China

Abstract. Soliton molecules, referred to as closely bounded solitons, have recently attracted considerable interest in both fundamental nonlinear physics research and refreshed application promises. To date, extensive efforts have been made on the generation of quadratic soliton molecules. These are soliton molecules whose formation exclusively involves second-order dispersion and Kerr nonlinearity. Here, for the first time, we demonstrate the realization of various third-order dispersion-supported soliton molecules, including vector dark–anti-dark solitons, vector anti-dark solitons, and vector anti-dark soliton molecules formed in a fiber laser with net cavity dispersion near the zero-group-velocity-dispersion point. High-order dispersion could greatly alter the internal soliton interaction within a soliton molecule. This finding could open exciting new avenues in soliton research.

Keywords: fiber laser; nonlinear optics; ultrafast fiber laser.

Received Jul. 27, 2024; revised manuscript received Oct. 22, 2024; accepted for publication Nov. 1, 2024; published online Nov. 23, 2024.

© The Authors. Published by SPIE and CLP under a Creative Commons Attribution 4.0 International License. Distribution or reproduction of this work in whole or in part requires full attribution of the original publication, including its DOI.

[DOI: [10.1117/1.AP.6.6.066005](https://doi.org/10.1117/1.AP.6.6.066005)]

1 Introduction

Solitons are localized wave packets that can propagate long distances in a nonlinear dispersive medium without changing their wave profiles.¹ Solitons have been observed in a wide range of physical systems in fluid dynamics, plasma physics, Bose–Einstein condensates, and biology. In optics, soliton formation in single-mode optical fibers has been extensively investigated. It is now well known that the solitons are governed by the nonlinear Schrödinger equation (NLSE), and depending on the sign of the fiber dispersion, either bright solitons² or dark solitons, represented as an intensity dip on a continuous-wave background,³ could be formed. Solitons can also interact with each other. While bright solitons could attract each other and form soliton molecules,⁴ dark solitons are known to experience only repulsive forces.^{5–7} Therefore, no dark soliton molecules can be formed in fibers unless specific stabilization schemes are applied.⁸ When birefringence of fibers is further considered, cross-phase modulation (XPM) between the orthogonally polarized light components could also result in vector soliton formation. Various forms of vector solitons have been theoretically predicted based on the coupled nonlinear Schrödinger equations (CNLSEs).^{9–19}

Strictly speaking, a fiber laser is essentially a dissipative nonlinear system whose dynamics is governed by the complex Ginzburg–Landau equation. However, under steady-state operation of a laser, the cavity losses are always balanced by the saturated gain; meanwhile, if the spectral bandwidth of the formed pulses is much narrower than that of the effective gain bandwidth, as is the case in our experiments, the gain bandwidth limiting effect could be neglected, and the dynamics of a fiber laser mimics those of the NLSE. Hence, fiber lasers are also routinely used as a platform to investigate the complex NLSE soliton dynamics. Not only the bright and dark solitons but also soliton molecules have been revealed in fiber lasers.^{20–22} In addition, NLSE types of vector bright,^{23–25} vector dark,^{26–28} and vector dark–bright^{29–31} solitons have also been experimentally observed in fiber lasers. In a more recent work, novel soliton molecules due to trapping between dark and bright solitons were further experimentally obtained in a fiber laser with net cavity dispersion near the zero-group velocity dispersion (ZGVD) point.³² When light propagates in a medium with near ZGVD, the higher order dispersion effects such as the third-order and/or fourth-order dispersion become a dominant influence rather than a perturbation. Theoretical studies have shown higher-order dispersions could give rise to novel new solitary wave solutions.^{33,34} A typical example is the formation of the anti-dark solitons, where because of the influence of the third-order

*Address all correspondence to Dingyuan Tang, tangdingyuan@sztu.edu.cn

dispersion, a dark soliton changes its profile from an intensity “dip” to an intensity “hump” on top of a CW background.^{35,36} Formation of scalar anti-dark solitons in a fiber laser has been experimentally demonstrated recently.³⁷ Using an intracavity spectral pulse shaper, Runge et al. experimentally demonstrated the pure fourth-order dispersion-supported solitons,³⁸ and Han et al. revealed the existence of pure-high-even-order dispersion-bound soliton complexes.³⁹

Based on higher-order CNLSEs, different research groups have theoretically predicted the existence of various forms of third-order dispersion supported vector solitons (TDSVSs), such as the vector anti-dark solitons,⁴⁰ vector dark–anti-dark solitons,⁴¹ and vector bright–anti-dark solitons.⁴² However, to the best of our knowledge, except for the experimental confirmation of vector bright–anti-dark solitons,⁴³ no experimental confirmation of the other TDSVSs has been reported. In this paper, we provide the first experimental evidence on these TDSVSs. Each type of the vector solitons can be interpreted as a (1+1) soliton molecule. Interaction between the soliton molecules is also experimentally investigated. We show that interaction between vector anti-dark solitons could produce attractive force, and as a result, a type of vector anti-dark soliton molecules could even be formed.

The importance of the work is twofold. On the one hand, for the first time, we believe, we have demonstrated various forms of third-order dispersion-supported soliton molecules (TDSSMs) in a fiber laser system. The result could expand the domain of Kerr cavity physics to near the ZGVD point regime, enabling

formation of higher-order soliton molecules. As the higher-order dispersion could greatly alter the internal soliton interaction within a soliton molecule, the results could thus trigger innovations on the collective excitations of higher-order supramolecular structures that could assist in understanding dynamical complexity in science; on the other hand, the cubic dispersion nature on the observed soliton molecules could grant them potential advantages in energy-width scaling [energy of anti-dark soliton scales like $E \propto \text{sech}^4(\tau)$, while for conventional bright solitons $E \propto \text{sech}^2(\tau)$; more details can be found in Sec. S1 of the [Supplementary Material](#)]; thus, the results could also present a superior alternative to conventional Kerr solitons that could benefit applications in fields of ultrafast lasers, spectroscopy, and optical communications.

2 Results

2.1 Experimental Setups

A schematic of the experimental setup is depicted in Fig. 1. Details on the setup and the parameters of the fibers used can be found in the Sec. S2 of the [Supplementary Material](#). A key factor for the current experiment is to ensure that the laser cavity has sufficiently small net cavity birefringence and dispersion. To this end, we have made use of both the cavity-dispersion and birefringence management techniques when constructing the laser. The fiber cavity consists of 3 m erbium-doped fiber (EDF), 8 m single-mode fiber (SMF), 0.2 m dispersion compensation fiber (DCF); the cavity has

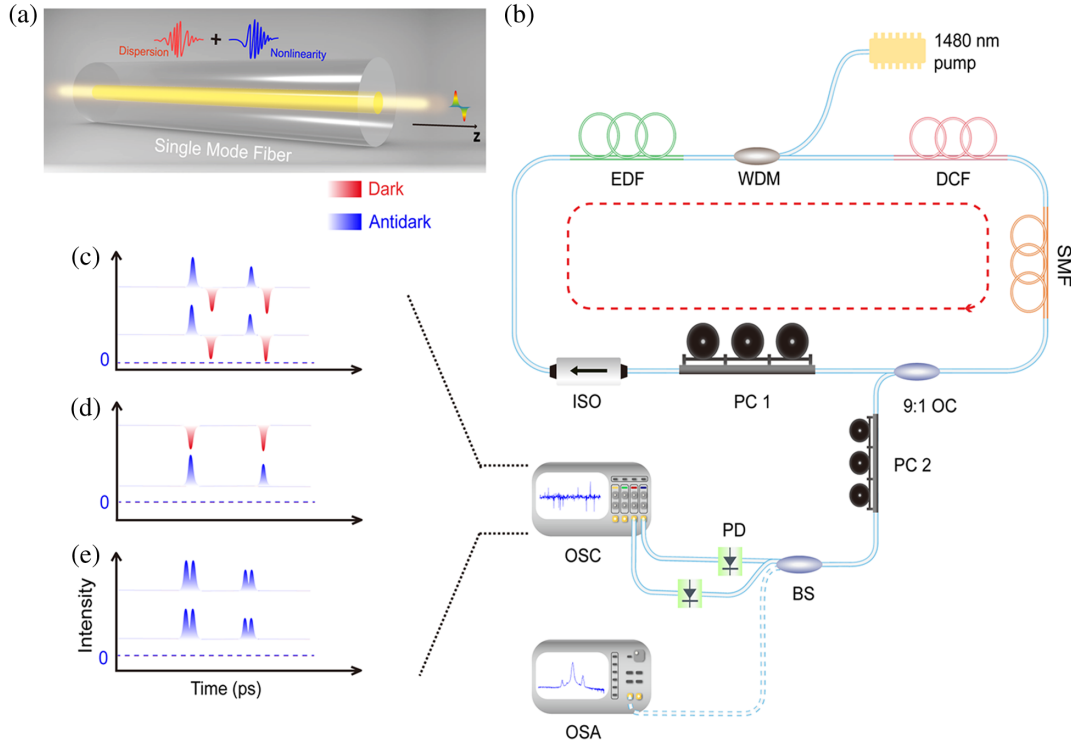


Fig. 1 Schematic of the experimental setup. (a) Illustration of an SMF. (b) The fiber ring laser configuration. EDF, erbium-doped fiber; DCF, dispersion compensation fiber; SMF, single-mode fiber; ISO, polarization-independent isolator; WDM, wavelength division multiplexer; OC, output coupler; BS, beam splitter; PD, photodetector; PC, polarization controller; OSC, oscilloscope; OSA, optical spectrum analyzer. (c)–(e) Schematic illustration on different states of the dark and anti-dark soliton molecules.

an averaged dispersion $\beta_{2,ave} = 0.01 \text{ ps}^2/\text{km}$. To check details of the soliton features, we perform time- and frequency-resolved measurement on the laser emission with a high-speed detection system consisting of a 40 GHz photodetector, a 33 GHz bandwidth real-time oscilloscope, and an optical spectrum analyzer.

2.2 Experimental Results

Theoretically, light propagation in a weakly birefringent SMF is described by the following coupled NLSEs:⁹

$$\begin{aligned} \frac{\partial u}{\partial z} &= +\delta \frac{\partial u}{\partial t} - \frac{i\beta_{2u}}{2} \frac{\partial^2 u}{\partial t^2} + i\gamma \left(|u|^2 + \frac{2}{3}|v|^2 \right) u + \frac{i}{3} \gamma v^2 u^*, \\ \frac{\partial v}{\partial z} &= -\delta \frac{\partial v}{\partial t} - \frac{i\beta_{2v}}{2} \frac{\partial^2 v}{\partial t^2} + i\gamma \left(|v|^2 + \frac{2}{3}|u|^2 \right) v + \frac{i}{3} \gamma u^2 v^*, \end{aligned} \quad (1)$$

where u and v are the normalized envelopes of the optical fields along the two orthogonal polarization directions, $\delta = \frac{1}{2} \left(\frac{1}{v_{gv}} - \frac{1}{v_{gu}} \right)$ is the inverse group velocity difference between them; β_{2u} and β_{2v} are the second-order dispersion coefficients of the fiber for the lights; and γ represents the averaged nonlinear coefficient of the fiber. If the birefringence of a fiber is too large because of the fast phase change of the light, the contribution of the last term averages to zero. In this case, one could also neglect the last term of the coupled equations, and the two

polarization components then become incoherently coupled. More details on the theoretical model can be found in Sec. S3 of the [Supplementary Material](#).

When light propagates inside a birefringent SMF, the cross-phase coupling between the orthogonally polarized light components may give rise to a two-component soliton state, referred to as a vector soliton. Depending on the strength of birefringence, sign, and magnitude of dispersion, different groups of vector solitons have been theoretically predicted. Figure 2 depicts the theoretical predictions on various vector soliton solutions based on the coupled NLSEs (CNLSEs). In Fig. 2, we have divided the GVD into six regions (I to VI). In different regions, CNLSEs support different soliton solutions, and the solitons have distinguishable characteristics. In a previous publication,³² we reported experimental observation of so-called 2+2 polyatomic soliton molecules (PSMs). Different from the conventional soliton molecules, PSMs constitute both dark and bright solitons. Here, we would like to emphasize that the solitons are actually formed in relatively large GVD regions, i.e., the dark solitons are formed in regime II, and the bright solitons are formed in regime V, where GVD and TOD are almost equal in magnitude, $GVD \approx TOD$, despite the fact that the net cavity dispersion is near the ZGVD point. Upon formation, the dark and bright solitons interact with each other, both along the same polarization and the orthogonal polarization axes, leading to the formation of complex soliton molecular

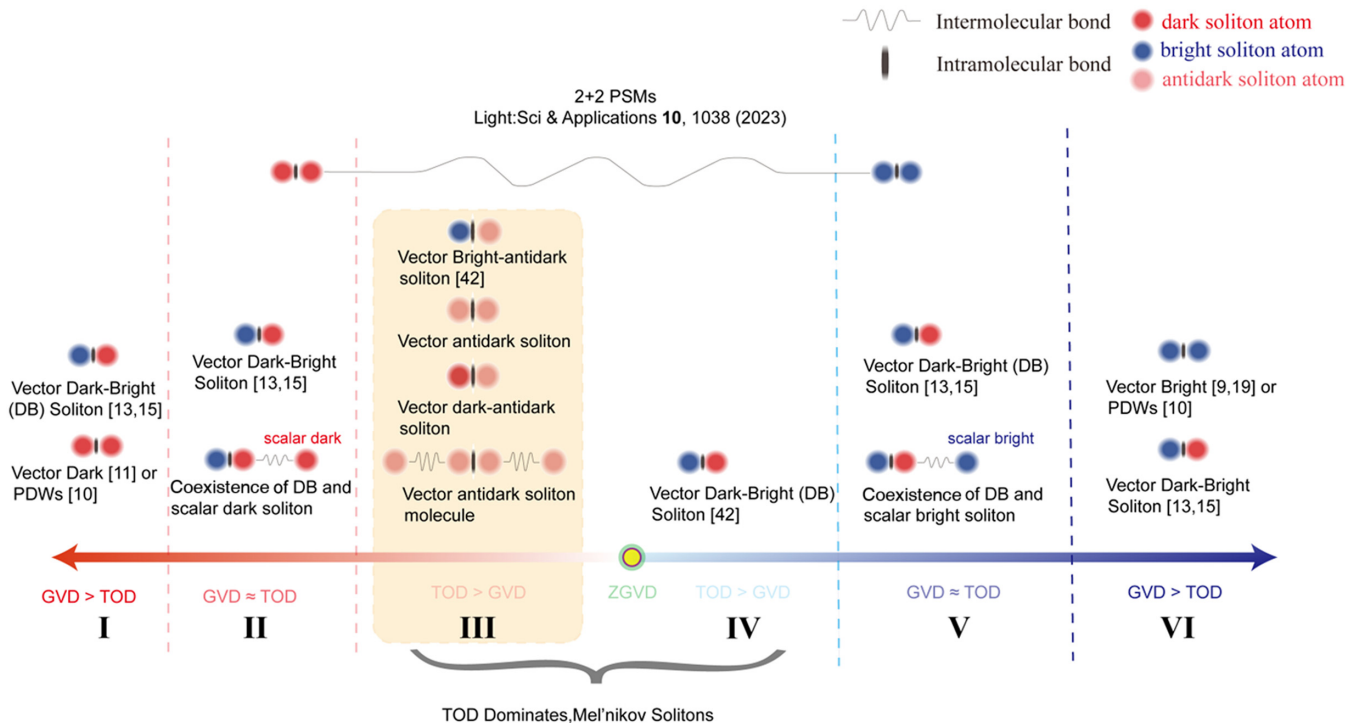


Fig. 2 Summary of theoretical predictions on various vector soliton solutions based on the CNLSEs or higher-order CNLSEs in different dispersion regions I to VI. Horizontal axis indicates magnitude of GVD (light to dark color corresponds to weak to strong GVD dispersion; red, normal GVD; blue, anomalous dispersion). Atomic representations of the cubic dispersion supported soliton molecules. Red-shaded circle: atomic representation for a dark soliton formed in the normal GVD regime; light red-shaded circle: atomic representation for an anti-dark soliton formed in the near ZGVD regime. Stripe notation: the intramolecular bond between orthogonally polarized solitons. Spring notations: the intermolecular bond between solitons with same polarization and different wavelengths.

structures. In this case, the effect of TOD is not obvious; therefore, the dynamics of PSMs could be fully governed by the CNLSEs. However, if we adjust the GVD closer to the ZGVD point, i.e., in region III and region IV, we will have to consider the effects of higher-order dispersion, i.e., the TOD. Recently, theoretical studies on higher-order dispersion-supported soliton structures have been a subject of great interest, but the experimental demonstrations of the solitons are still rare. Therefore, in this paper, we focus on solitons formed in region III and provide further experimental results on the TOD-supported soliton structures.

When operating the laser in a relatively low nonlinearity regime, e.g., injecting a pump power of ~ 20 dBm into the cavity, the laser always emits CW along the two orthogonal polarization directions. As the pump power is slowly increased to 21 dBm, a state as shown in Fig. 3 could generally be obtained. Figures 3(a) and 3(b) show the evolution of the polarization-resolved laser emissions with the cavity round trips. Figure 3(c) is a snapshot of the oscilloscope traces, and Fig. 3(d) is the corresponding polarization-resolved optical spectra. Multiple pairs of vector dark pulses are clearly visible in the cavity and move stably with the cavity round trips. The appearance of the Kelly sidebands further supports the fact that they are dark solitons formed in the laser. The central wavelength of the dark solitons polarized along the two orthogonally polarized directions is slightly different, indicating that they are incoherently coupled. Therefore, it shows an incoherently coupled vector dark-soliton emission state of the laser. A similar state of fiber laser emissions was also reported in Ref. 27.

The results presented in Fig. 3 demonstrate that the net cavity dispersion of the fiber laser is in the normal dispersion regime. In the same dispersion region, we have also obtained vector dark–bright solitons like those reported in Ref. 30. The results are well in agreement with the theoretical predictions of the incoherently coupled NLSEs.¹⁵

Starting from a state as shown in Fig. 3, keep other laser parameters unchanged and carefully tune the intracavity PC paddles so that the central wavelengths of the laser emissions

move closer to the ZGVD point of the cavity, which corresponds to enhancing the TOD effect (we introduce a spectral analysis method to quantify the TOD in our experiments; more details can be found in Sec. S2.4 of the [Supplementary Material](#)). A state of laser emission as shown in Fig. 4 could be further obtained. Different from the state shown in Fig. 3, where incoherently coupled dark–dark solitons are observed, in the current state incoherently coupled dark–anti-dark solitons are obtained. Although at first sight it looks like a vector dark–bright soliton emission state as reported in Ref. 30, carefully comparing the polarization-resolved optical spectra of the state with those shown in Fig. 3(d), where only vector dark solitons are present, it seems they exhibit essentially similar characteristics, except that the optical spectra have become broader. The result suggests that the bright pulses observed in the state are in fact anti-dark solitons rather than bright solitons. It is necessary to further point out that in the same dispersion region, we have also experimentally observed vector anti-dark–bright solitons, as those reported in Ref. 43. Such a vector soliton state is a typical third-order dispersion-supported effect, which could even be analytically solved from the incoherently coupled high-order NLSEs.⁴² The observation of the vector anti-dark–bright solitons clearly suggests that the net cavity dispersion of our laser is very close to the ZGVD point.

In addition to vector dark–anti-dark and anti-dark–bright solitons, depending on the detailed laser operation conditions, in the same dispersion region, we have also observed several other novel vector soliton states. Figure 5 shows, for example, a state where multiple pairs of vectorial anti-dark solitons are formed. The vector anti-dark solitons coexist with the vector dark solitons in the cavity. If we trigger the oscilloscope traces with one pair of the anti-dark solitons, other pairs of the vector anti-dark and vector dark solitons still move in the cavity, undergoing collisions, suggesting that they move with different velocities in the cavity. The experimental result shows that not only scalar anti-dark solitons but also vector anti-dark solitons could be formed. To confirm vector anti-dark soliton formation, we also numerically simulated such a state of our fiber laser in Sec. S4 of the [Supplementary Material](#) using a model presented in Sec. S3 of the [Supplementary Material](#).

Figure 5(b) shows the polarization-resolved optical spectra of Fig. 5(a). Compared with those shown in Fig. 3(d), they exhibit again essentially similar characteristics. We emphasize that the vector anti-dark and vector dark solitons in Fig. 5(a) have always displayed comparable pulse width. Under the influence of third-order dispersion, experimentally we also observed another interesting state, as shown in Fig. 6, where in addition to the formation of vector dark and anti-dark solitons, vector dark–anti-dark solitons (marked by the yellow shaded area in Fig. 6) are also simultaneously formed. The various types of vector solitons coexist in the cavity and interact with each other. Although previous theoretical studies have revealed that the interaction between scalar dark and anti-dark solitons along the same polarization is always repulsive and travels in opposite directions, we also verified this feature experimentally in Sec. S2.3 of the [Supplementary Material](#). In Fig. 6, we found that under cross-polarization coupling, trapping between orthogonally polarized dark and anti-dark solitons could become possible, and consequently, vector dark–anti-dark solitons are formed, as shown in Figs. 4 and 6. We have also numerically confirmed this trapping state in Sec. S5 of the [Supplementary Material](#).

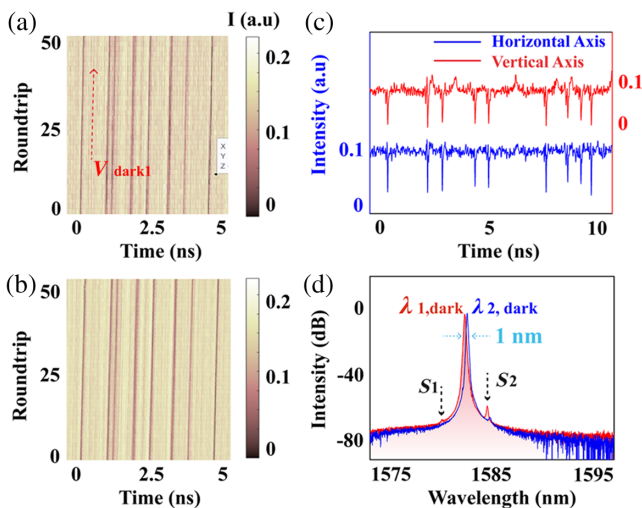


Fig. 3 A state of vector dark soliton emission. (a), (b) Evolutions of the polarization-resolved dark solitons with the cavity round trips. (c) Polarization-resolved laser emissions. (d) The corresponding optical spectra of (a) and (b).

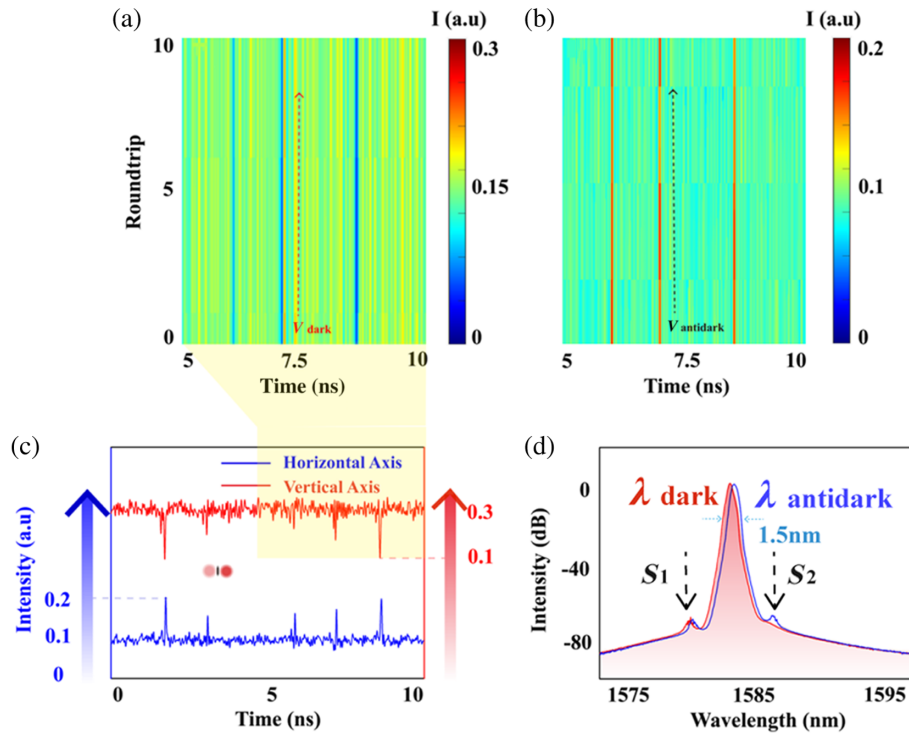


Fig. 4 A state of vector dark-anti-dark soliton emission. (a), (b) Evolutions of vector dark and anti-dark solitons. (c) Polarization-resolved laser emissions. (d) The corresponding optical spectra of (c).

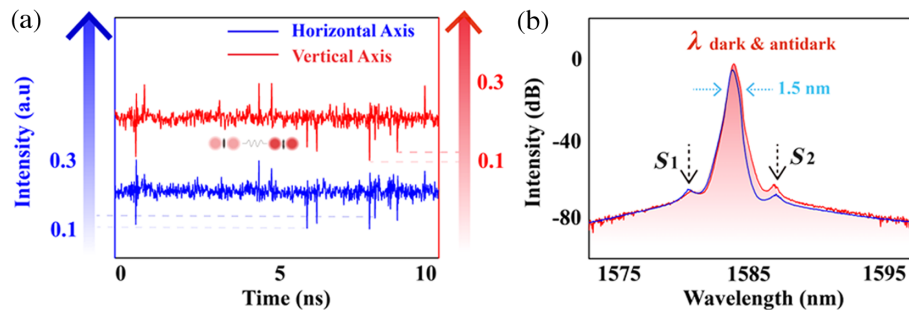


Fig. 5 A state of coexistence of vector dark and vector anti-dark solitons. (a) Polarization-resolved laser emissions. (b) The optical spectra of (a).

Keeping the laser emission wavelengths unchanged as in Fig. 5 but increasing the pump power, the spectral bandwidths of the solitons further broaden, and the soliton pulse widths narrow down. Limited by the resolution of our detection system, eventually, as the pump power increases to 23 dBm, the vector dark solitons no longer become detectable. In this case, the oscilloscope traces only display the anti-dark vector solitons, as shown in Fig. 7. Considering this detection limitation, the appearance of anti-dark solitons could also provide us with an opportunity to check the occurrence of dark solitons in the system. Meanwhile, as anti-dark solitons are transformed from the dark solitons as a result of influence by third-order dispersion, and the dark, anti-dark solitons normally have comparable pulse width, in this context, we can estimate the pulse width of dark solitons based on the measured pulse width of anti-dark solitons.

The vector anti-dark solitons shown in Figs. 5–7 display distinguishable pulse heights, which is a typical feature of the incoherently coupled vector solitons of the CNLSEs. By fixing the laser pump power at a high level, e.g., 23 dBm, and carefully fine-tuning the intracavity PC paddles, occasionally a kind of vector anti-dark soliton emission state as shown in Fig. 8 could also be obtained. Different from the vector anti-dark solitons shown in Figs. 5–7, all the vector anti-dark solitons formed in the cavity have almost the same pulse height; in addition, they are very stable in the cavity. We suspect such a state could be formed due to the coherent cross-polarization coupling between the two orthogonally polarized laser emission components. Experimentally, we also measured intracavity power and the autocorrelation trace for the coherently coupled anti-dark solitons. With the intracavity power of 40 mW, the autocorrelation trace is obtained as shown in Fig. 8(b). If a sech-form pulse shape is

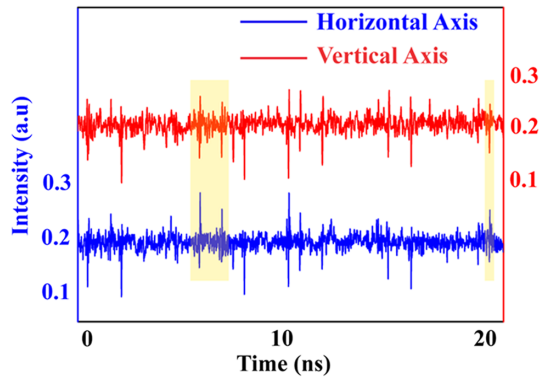


Fig. 6 A state of vector dark–anti-dark solitons and the coexistence of vector dark, anti-dark, and vector dark–anti-dark solitons. Yellow shaded area: vector dark–anti-dark solitons, dark (anti-dark) solitons polarized along the vertical (horizontal) axis.

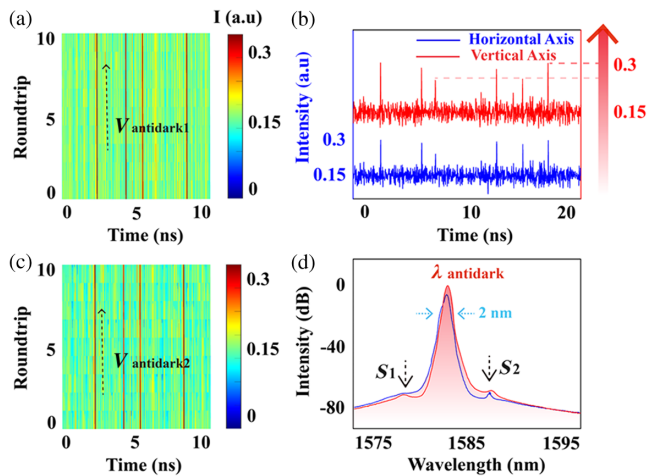


Fig. 7 A state of “pure” vector anti-dark soliton emission. (a), (c) Evolution of anti-dark solitons along two orthogonal polarization axes, respectively. (b) Polarization-resolved laser emissions. (d) The optical spectra of (a) and (c).

assumed, the pulse width is estimated to be 1.2 ps. In previous studies, we have shown that under coherent cross-polarization coupling, only the vector black solitons, i.e., dark solitons with π phase jump and zero minimum intensity, will be formed, and the formed vector black solitons have excellent stability.²⁸

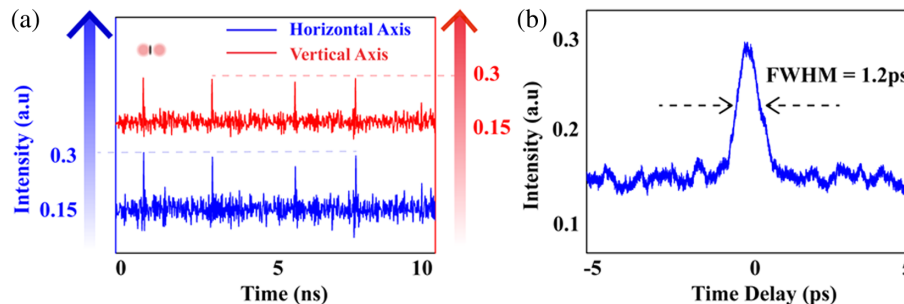


Fig. 8 (a) A state of coherently coupled vector anti-dark soliton emission. (b) Experimentally measured autocorrelation trace.

Therefore, it is highly believable that under coherent cross-polarization coupling, the anti-dark solitons could also display a similar feature. If this is the case, the coherently coupled vector anti-dark solitons would be useful for large energy ultrashort pulse generation. Compared with the conventional NLSE bright solitons, coherently cross-polarization-coupled anti-dark solitons would not only have improved soliton stability over the bright solitons but also better pulse energy scaling: the energy-pulse width of the anti-dark solitons scales like $E \propto \text{sech}^4(\tau)$, while that of the conventional bright solitons is $E \propto \text{sech}^2(\tau)$ (more derivation details can be found in Sec. S1 of the [Supplementary Material](#)). Therefore, the coherently coupled vector anti-dark solitons could be a superior alternative to conventional bright solitons for applications in fields of ultrafast lasers, spectroscopy, and optical communications.

Despite the fact that interactions are repulsive between scalar dark solitons and between scalar dark and anti-dark solitons, recent theoretical studies have shown that the interaction between anti-dark solitons contrasts starkly with the dark solitons. In particular, by means of different mathematical methods, different research groups have theoretically predicted the coexistence of dark and anti-dark solitons based on the coupled high-order NLSEs.^{40–42,44} Interestingly, it was shown that anti-dark solitons could experience attractive interactions that could lead to formation of anti-dark soliton molecules. In our experiment, we indeed have observed such an anti-dark soliton molecule emission state, as presented in Fig. 9. Like the state shown above in Fig. 5(a), multiple pairs of incoherently coupled vector dark and anti-dark solitons are simultaneously formed in the laser. However, different from the vector dark and anti-dark solitons observed in Fig. 5(a), where the dark and anti-dark solitons have comparable pulse widths, here all the vector anti-dark solitons have obviously broader pulse width than the vector dark solitons. Figure 9(b) is the corresponding polarization-resolved optical spectra of Fig. 9(a). The spectra of the solitons are strongly modulated, which is a characteristic of bound solitons with a very close temporal soliton separation. Combining the information presented in Figs. 9(a) and 9(b), we conclude that the broad anti-dark pulses could be a bound state of the anti-dark solitons. Indeed, Wang et al. theoretically predicted a type of spatiotemporal N-anti-dark soliton solutions based on a high-dimensional KdV equation.⁴⁵ Both anti-dark triplets and quartets are predicted. It is shown that the interaction between anti-dark solitons could generate an attractive force between them. This matches well with our simulation results, shown in Sec. S6 of the [Supplementary Material](#). It is notable that as we shift the central wavelength of laser emission much closer

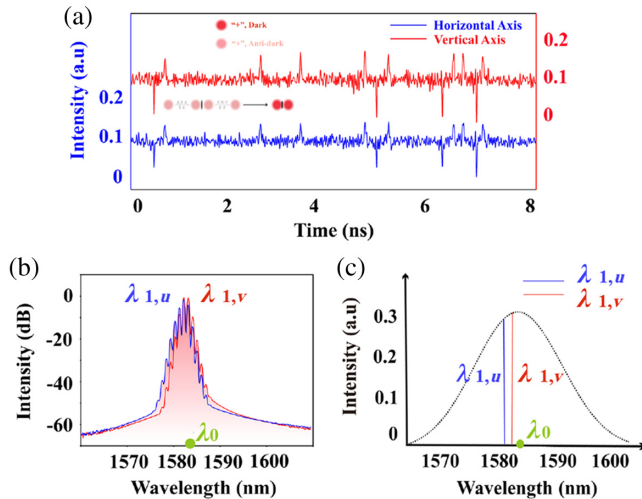


Fig. 9 A state of coexistence of vector dark and vector anti-dark soliton molecules. (a) Polarization-resolved laser emissions. (b) Corresponding optical spectra of (a). (c) Schematic illustration of the central wavelengths of vector dark and anti-dark solitons in normal dispersion regime. λ_0 , position of ZGVD point; $\lambda_{1,u}$, wavelength of the dark and anti-dark solitons formed along horizontal axis; $\lambda_{1,v}$, wavelength of the dark and anti-dark solitons formed along vertical axis.

to the ZGVD point, the TOD effect will be enhanced; consequently, the TOD could alter the dynamics of the anti-dark solitons. On the one hand, with the enhancement of TOD, the onset of anti-dark solitons becomes easier; on the other hand, the relatively large TOD will bring in oscillation tails on the anti-dark soliton pulse envelopes (we have numerically verified this phenomenon in Fig. S15 in the [Supplementary Material](#)). Moreover, we found that the signs of TOD will result in oscillation tails appearing in opposite directions on the anti-dark soliton envelope, as shown in Fig. S16 in the [Supplementary Material](#). More simulation details can be found in Sec. S5 of the [Supplementary Material](#). Furthermore, depending on the phase relationship between oscillation tails, the interaction dynamics between anti-dark solitons could be greatly altered; for instance, in-phase oscillation could enhance both long-range and short-range interactions between them, leading to formation of anti-dark soliton molecules, as shown in Fig. 9. It is worth noting that the dispersive Fourier transform (DFT) technique has been widely used to study fast transient soliton phenomena.⁴⁶ However, applying the technique to investigate the internal dynamics of anti-dark soliton molecules formed under third-order dispersion remains challenging. The difficulty arises from the thresholdless nature of small-amplitude dark soliton formation. Unlike bright solitons in mode-locked lasers,⁴⁶ where the number of solitons in the laser cavity can be effectively controlled, dark solitons (or anti-dark solitons) tend to form in large numbers simultaneously. To retrieve accurate instantaneous spectral information of a pulse using the DFT technique, it is crucial that the pulses must be well separated in the time domain; otherwise linear propagation through the DFT fiber would cause significant overlap in the spectra of the pulses, rendering the technique ineffective. Therefore, finding a way to effectively control the generation of dark and/or anti-dark solitons is essential before applying the DFT technique. A potential approach could be through the induced soliton technique. If anti-dark solitons

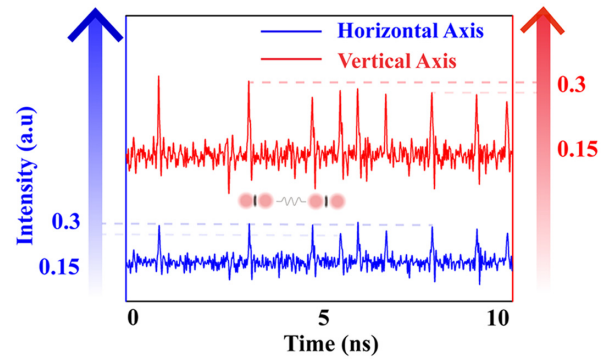


Fig. 10 A state of laser emission where only the vector anti-dark soliton molecules are detectable.

could be induced through cross-polarization coupling under effect of third-order dispersion, one would be able to control the anti-dark soliton generation through control of the bright soliton. Many research groups have proposed different techniques to precisely control the temporal and spectral spacing between bright solitons in soliton molecules.⁴⁷

Based on the experimentally measured spectral fringe period $\Delta\nu = 0.18$ THz, the temporal separation between the anti-dark solitons in an anti-dark soliton molecule is estimated to be 5.56 ps. Once formed, the vector anti-dark soliton molecules and vector dark solitons move with different group velocities in the cavity and collide with each other. From a state as shown in Fig. 9, if the pump power is further slowly increased, again, the vector dark solitons will become undetectable. Consequently, the oscilloscope will display only “vector anti-dark soliton molecule” emissions, as shown in Fig. 10.

Finally, it is worth noting that the observed vector dark–anti-dark, vector anti-dark solitons could also be interpreted as $(1 + 1)$ TDSSMs, while the vector anti-dark soliton molecules can be described as more complex $(N + N)$ soliton molecules, where N represents the number of one-component anti-dark solitons within each anti-dark soliton molecule. Notably, the inclusion of vectorial soliton components in these molecules significantly enriches the binding schemes of optical molecules. For instance, in addition to intermolecular bonding (same polarization interaction), we can now also manipulate intramolecular bonding (cross-polarization interaction). These vector soliton molecules offer a greatly increased degree of freedom, holding promise for applications in advanced encoding techniques. We stress this is the first experimental observation of vector anti-dark soliton molecules in any physical system. In view of the fact that third-order dispersion strongly affects the internal degrees of freedom of soliton molecules, we believe the demonstration of anti-dark soliton molecules is of great significance in providing deeper understanding on soliton interaction in higher-order dispersion-supported soliton molecular complexes.

3 Conclusion

In summary, we have shown experimental evidence of various forms of cubic dispersion-supported solitons and soliton molecules by operating a fiber laser with cavity dispersion near the ZGVD point. This opens unprecedented possibilities to control and manipulate the collective excitations of the dark and anti-dark solitons, enabling the generation of multiple types of vector

solitons as well as studying their mutual interactions. The scope of our findings is not limited to the nonlinear optics but may provide insights into other physical systems, such as fluid mechanics and plasma physics, where these features are crucial. The concept of cubic dispersion-supported soliton molecules is not only of significance from the fundamental research point of view but also has impact at the applied level. Recent interest in soliton molecules in both microresonator and other guided wave systems with applications in frequency combs, communications, and ultrafast lasers could also benefit from exploring higher-order soliton molecules in their systems.^{48,49}

Disclosures

The authors declare that there are no financial interests, commercial affiliations, or other potential conflicts of interest that could have influenced the objectivity of this research or the writing of this paper.

Codes and Data Availability

The data supporting this article are available from the corresponding author upon reasonable request.

Acknowledgments

This project was supported by the Education Department of the Guangdong Province (Grant No. 2022ZDJS116); the National Science Foundation of Top Talent of SZTU (Grant No. GDRC202302); the Agency for Science, Technology and Research, Singapore (Grant No. IRG M21K2c0109); and the Singapore Ministry of Education (Grant No. RG114/21).

References

1. A. C. Scott, F. Y. F. Chu, and D. W. McLaughlin, "The soliton: a new concept in applied science," *Proc. IEEE* **61**(10), 1443–1483 (1973).
2. A. Hasegawa and F. Tappert, "Transmission of stationary nonlinear optical pulses in dispersive dielectric fibers. I. Anomalous dispersion," *Appl. Phys. Lett.* **23**(3), 142–144 (1973).
3. A. Hasegawa and F. Tappert, "Transmission of stationary nonlinear optical pulses in dispersive dielectric fibers. II. Normal dispersion," *Appl. Phys. Lett.* **23**(4), 171–172 (1973).
4. M. Segev and G. Stegeman, "Self-trapping of optical beams: spatial solitons," *Phys. Today* **51**(8), 42–48 (1998).
5. Y. S. Kivshar and B. Luther-Davies, "Dark optical solitons: physics and applications," *Phys. Rep.* **298**(2-3), 81–197 (1998).
6. D. J. Frantzeskakis, "Dark solitons in atomic Bose–Einstein condensates: from theory to experiments," *J. Phys. A: Math. Theor.* **43**(21), 213001 (2010).
7. W. Zhao and E. Bourkoff, "Interactions between dark solitons," *Opt. Lett.* **14**(24), 1371–1373 (1989).
8. E. A. Ostrovskaya et al., "Interactions between vector solitons and solitonic gluons," *Opt. Lett.* **24**(5), 327–329 (1999).
9. C. Menyuk, "Nonlinear pulse propagation in birefringent optical fibers," *IEEE J. Quantum Electron.* **23**(2), 174–176 (1987).
10. M. Haelterman and A. Sheppard, "Polarization domain walls in diffractive or dispersive Kerr media," *Opt. Lett.* **19**(2), 96–98 (1994).
11. Y. S. Kivshar and S. K. Turitsyn, "Vector dark solitons," *Opt. Lett.* **18**(5), 337–339 (1993).
12. V. V. Afanasjev, "Soliton polarization rotation in fiber lasers," *Opt. Lett.* **20**(3), 270–272 (1995).
13. D. N. Christodoulides, "Black and white vector solitons in weakly birefringent optical fibers," *Phys. Lett. A* **132**(8-9), 451–452 (1988).
14. S. T. Trillo et al., "Optical solitary waves induced by cross-phase modulation," *Opt. Lett.* **13**(10), 871–873 (1988).
15. M. Lisak et al., "Symbiotic solitary-wave pairs sustained by cross-phase modulation in optical fibers," *J. Opt. Soc. Am. B* **7**(5), 810–814 (1990).
16. Y. S. Kivshar, "Stable vector solitons composed of bright and dark pulses," *Opt. Lett.* **17**(19), 1322–1324 (1992).
17. V. V. Afanasjev et al., "Dynamics of coupled dark and bright optical solitons," *Opt. Lett.* **14**(15), 805–807 (1989).
18. A. V. Buryak et al., "Coupling between dark and bright solitons," *Phys. Lett. A* **215** (1-2), 57–62 (1996).
19. N. N. Akhmediev et al., "Phase-locked stationary soliton states in birefringent nonlinear optical fibers," *J. Opt. Soc. Am. B* **12** (3), 434–439 (1995).
20. W. He et al., "Formation of optical supramolecular structures in a fibre laser by tailoring long-range soliton interactions," *Nat. Commun.* **10**(1), 5756 (2019).
21. Z. Q. Wang et al., "Optical soliton molecular complexes in a passively mode-locked fibre laser," *Nat. Commun.* **10** (1), 830 (2019).
22. Y. Y. Luo et al., "Real-time dynamics of soliton triplets in fiber lasers," *Photonics Res.* **8**(6), 884–891 (2020).
23. M. N. Islam et al., "Soliton trapping in birefringent optical fibers," *Opt. Lett.* **14**(18), 1011–1013 (1989).
24. D. Y. Tang et al., "Observation of high-order polarization-locked vector solitons in a fiber laser," *Phys. Rev. Lett.* **101**(15), 153904 (2008).
25. S. T. Cundiff et al., "Observation of polarization-locked vector solitons in an optical fiber," *Phys. Rev. Lett.* **82**(20), 3988–3991 (1999).
26. P. Zhang et al., "Self-starting triple-wavelength vector dark soliton with a bismuth-doped fiber saturable absorber," *Opt. Lett.* **46**(14), 3336–3339 (2021).
27. G. D. Shao et al., "Vector dark solitons in a single mode fibre laser," *Laser Phys. Lett.* **16**(8), 085110 (2019).
28. X. Hu et al., "Coherently coupled vector black solitons in a quasi-isotropic cavity fiber laser," *Opt. Lett.* **45**(23), 6563–6566 (2020).
29. J. Ma et al., "Observation of dark-bright vector solitons in fiber lasers," *Opt. Lett.* **44**(9), 2185–2188 (2019).
30. X. Hu et al., "Observation of incoherently coupled dark-bright vector solitons in single-mode fibers," *Opt. Express* **27**(13), 18311–18317 (2019).
31. X. Hu et al., "Polarization domain splitting and incoherently coupled dark-bright vector soliton formation in single mode fiber lasers," *J. Opt. Soc. Am. B* **38**(1), 24–29 (2020).
32. X. Hu et al., "Novel optical soliton molecules formed in a fiber laser with near-zero net cavity dispersion," *Light: Sci. Appl.* **12**, 38 (2023).
33. J. P. Lourdesamy et al., "Polychromatic soliton molecules," arXiv:2007.01351 (2020).
34. C. M. de Sterke, "Pure-quartic solitons and their generalizations—theory and experiments," *APL Photonics* **6**(9), 6689–6699 (2021).
35. Y. S. Kivshar and V. V. Afanasjev, "Dark optical solitons with reverse-sign amplitude," *Phys. Rev. A* **44**(3), R1446–R1449 (1991).
36. Y. S. Kivshar, "Dark optical solitons near the zero-dispersion wavelength," *Opt. Lett.* **16**(12), 892–894 (1991).
37. J. Guo, "Anti-dark solitons in a single mode fiber laser," *Phys. Lett. A* **395**, 127226 (2021).
38. A. F. J. Runge et al., "The pure-quartic soliton laser," *Nat. Photonics* **14**(8), 492–497 (2020).
39. Y. Han et al., "Pure-high-even-order dispersion bound solitons complexes in ultra-fast fiber lasers," *Light Sci. Appl.* **13**(1), 101 (2024).
40. Y. Zhang, "Interactions of vector anti-dark solitons for the coupled nonlinear Schrödinger equation in inhomogeneous fibers," *Nonlinear Dyn.* **94**(2), 1351–1360 (2018).
41. M. Li et al., "Bound-state dark/antidark solitons for the coupled mixed derivative nonlinear Schrödinger equations in optical fibers," *Eur. Phys. J. D* **66**, 297 (2012).
42. D. J. Frantzeskakis, "Vector solitons supported by the third-order dispersion," *Phys. Lett. A* **285**(5-6), 363–367 (2001).

43. J. Guo et al., “Observation of vector solitons supported by third-order dispersion,” *Phys. Rev. A* **99**(6), 061802(R) (2019).
44. M. Li et al., “Dark and anti-dark vector solitons of the coupled modified nonlinear Schrödinger equations from the birefringent optical fibers,” *Eur. Phys. J. D* **59**(2), 279–289 (2010).
45. X. Wang and J. Wei, “Antidark solitons and soliton molecules in a $(3 + 1)$ -dimensional nonlinear evolution equation,” *Nonlinear Dyn.* **102**(1), 363–377 (2020).
46. Y. D. Cui et al., “Dichromatic ‘breather molecules’ in a mode-locked fiber laser,” *Phys. Rev. Lett.* **130**(15), 153801 (2023).
47. J. P. Lourdesamy et al., “Spectrally periodic pulses for enhancement of optical nonlinear effects,” *Nat. Phys.* **18**(1), 59–66 (2022).
48. W. Weng et al., “Heteronuclear soliton molecules in optical microresonators,” *Nat. Commun.* **11**(1), 2402 (2020).
49. B. Q. Li and Y. L. Ma, “Optical soliton resonances and soliton molecules for the Lakshmanan–Porsezian–Daniel system in nonlinear optics,” *Nonlinear Dyn.* **111**(7), 6689–6699 (2023).

Xiao Hu received her PhD from Nanyang Technological University (NTU) in 2022. Since graduating, she has continued her postdoctoral research at NTU. Notably, her research has made significant original contributions in the field of ultrafast optics and optical solitons, pioneering multiple research directions, including vector solitons, bright-dark solitons, topological solitons, and dissipative solitons.

Dingyuan Tang is currently a chair professor at Shenzhen Technology University, China. He received his PhD in physics from Hanover University, Germany, in 1993. Prof. His research interests include laser physics and technique, ultrafast optics, nonlinear fiber optics, and ceramic laser materials. He has published over 500 international journal papers and was among the world's top 1% highly cited researchers in the field of physics (or cross-field) from 2017 to 2023.

Biographies of the other authors are not available.